

# Aerodynamic Inverse Design and Shape Optimization via Control Theory

Antony Jameson<sup>1</sup>

<sup>1</sup>Thomas V. Jones Professor of Engineering  
Department of Aeronautics & Astronautics  
Stanford University

SciTech 2015  
January 5, 2015

- 1 **Introduction**
  - Introduction
  - Lighthill's Method
  - Control Theory Approach to Design

- 2 **Numerical Formulation**
  - Design using the Euler Equations
  - Sobolev Inner Product

- 3 **Design Process**
  - Design Process Outline
  - Drag Minimization
  - Inverse Design
  - P51 Racer
  - Reduced Sweep: Design for the CRM
  - Low Sweep Wing Design
  - Natural Laminar Wing
  - Numerical Wind Tunnel

- 4 **Appendix**
  - Design using the Transonic Potential Flow Equation







# LIGHTHILL'S METHOD























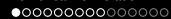






# Advantages

- The advantage is that (6) is independent of  $\delta w$ , with the result that the gradient of  $I$  with respect to an arbitrary number of design variables can be determined without the need for additional flow-field evaluations.
- The cost of solving the adjoint equation is comparable to that of solving the flow equations. Thus the gradient can be determined with roughly the computational costs of two flow solutions, independently of the number of design variables, which may be infinite if the boundary is regarded as a free surface.
- When the number of design variables becomes large, the computational efficiency of the control theory approach over traditional approach, which requires direct evaluation of the gradients by individually varying each design variable and recomputing the flow fields, becomes compelling.



# DESIGN USING THE EULER EQUATIONS



## Design using the Euler Equations

A variation in the geometry now appears as a variation  $\delta S_{ij}$  in the metric coefficients. The variation in the residual is

$$\delta R = \frac{\partial}{\partial \xi_i} (\delta S_{ij} f_j) + \frac{\partial}{\partial \xi_i} \left( S_{ij} \frac{\partial f_j}{\partial w} \delta w \right) \quad (9)$$

and the variation in the cost  $\delta I$  is augmented as

$$\delta I - \int_D \psi^T \delta R d\xi \quad (10)$$

which is integrated by parts to yield

$$\delta I - \int_B \psi^T n_i \delta F_i d\xi_B + \int_D \frac{\partial \psi^T}{\partial \xi} (\delta S_{ij} f_j) d\xi + \int_D \frac{\partial \psi^T}{\partial \xi_i} S_{ij} \frac{\partial f_j}{\partial w} \delta w d\xi$$

# Design using the Euler Equations

For simplicity, it will be assumed that the portion of the boundary that undergoes shape modifications is restricted to the coordinate surface  $\xi_2 = 0$ . Then equations for the variation of the cost function and the adjoint boundary conditions may be simplified by incorporating the conditions

$$n_1 = n_3 = 0, \quad n_2 = 1, \quad \mathcal{B}_\xi = d\xi_1 d\xi_3,$$

so that only the variation  $\delta F_2$  needs to be considered at the wall boundary. The condition that there is no flow through the wall boundary at  $\xi_2 = 0$  is equivalent to

$$U_2 = 0, \quad \text{so that} \quad \delta U_2 = 0$$

when the boundary shape is modified. Consequently the variation of the inviscid flux at the boundary reduces to

$$\delta F_2 = \delta p \begin{Bmatrix} 0 \\ S_{21} \\ S_{22} \\ S_{23} \\ 0 \end{Bmatrix} + p \begin{Bmatrix} 0 \\ \delta S_{21} \\ \delta S_{22} \\ \delta S_{23} \\ 0 \end{Bmatrix}. \quad (11)$$

## Design using the Euler Equations

In order to design a shape which will lead to a desired pressure distribution, a natural choice is to set

$$I = \frac{1}{2} \int_{\mathcal{B}} (p - p_d)^2 dS$$

where  $p_d$  is the desired surface pressure, and the integral is evaluated over the actual surface area. In the computational domain this is transformed to

$$I = \frac{1}{2} \iint_{\mathcal{B}_w} (p - p_d)^2 |S_2| d\xi_1 d\xi_3,$$

where the quantity

$$|S_2| = \sqrt{S_{2j} S_{2j}}$$

denotes the face area corresponding to a unit element of face area in the computational domain.

















# The Need for a Sobolev Inner Product in the Definition of the Gradient

Note that  $g$  is a function of  $y, y', y''$ ,

$$g = g(y, y', y'')$$

In the well known case of the Brachistone problem, for example, which calls for the determination of the path of quickest descent between two laterally separated points when a particle falls under gravity,

$$F(y, y') = \sqrt{\frac{1 + y'^2}{y}}$$

and

$$g = -\frac{1 + y'^2 + 2yy''}{2[y(1 + y'^2)]^{3/2}}$$

It can be seen that each step

$$y^{n+1} = y^n - \lambda^n g^n$$

reduces the smoothness of  $y$  by two classes. Thus the computed trajectory becomes less and less smooth, leading to instability.



# The Need for a Sobolev Inner Product in the Definition of the Gradient

In order to prevent this we can introduce a weighted Sobolev inner product

$$\langle u, v \rangle = \int (uv + \epsilon u'v') dx$$

where  $\epsilon$  is a parameter that controls the weight of the derivatives. We now define a gradient  $\bar{g}$  such that  $\delta I = \langle \bar{g}, \delta y \rangle$ . Then we have

$$\begin{aligned} \delta I &= \int (\bar{g}\delta y + \epsilon \bar{g}'\delta y') dx \\ &= \int \left( \bar{g} - \frac{\partial}{\partial x} \epsilon \frac{\partial \bar{g}}{\partial x} \right) \delta y dx \\ &= (g, \delta y) \end{aligned}$$

where

$$\bar{g} - \frac{\partial}{\partial x} \epsilon \frac{\partial \bar{g}}{\partial x} = g$$

and  $\bar{g} = 0$  at the end points.

# The Need for a Sobolev Inner Product in the Definition of the Gradient

Therefore  $\bar{g}$  can be obtained from  $g$  by a smoothing equation.

Now the step

$$y^{n+1} = y^n - \lambda^n \bar{g}^n$$

gives an improvement

$$\delta I = -\lambda^n \langle \bar{g}^n, \bar{g}^n \rangle$$

but  $y^{n+1}$  has the same smoothness as  $y^n$ , resulting in a stable process.



# OUTLINE OF THE DESIGN PROCESS

# Outline of the Design Process

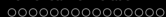
The design procedure can finally be summarized as follows:

- 1 Solve the flow equations for  $\rho$ ,  $u_1$ ,  $u_2$ ,  $u_3$  and  $p$ .
- 2 Solve the adjoint equations for  $\psi$  subject to appropriate boundary conditions.
- 3 Evaluate  $\mathcal{G}$  and calculate the corresponding Sobolev gradient  $\overline{\mathcal{G}}$ .
- 4 Project  $\overline{\mathcal{G}}$  into an allowable subspace that satisfies any geometric constraints.
- 5 Update the shape based on the direction of steepest descent.
- 6 Return to 1 until convergence is reached.









# Computational Cost★

## Cost of Search Algorithm

Steepest Descent	$\mathcal{O}(N^2)$	Steps
Quasi-Newton	$\mathcal{O}(N)$	Steps
Smoothed Gradient	$\mathcal{O}(K)$	Steps

Note:  $K$  is independent of  $N$ .

★: "Studies of Alternative Numerical Optimization Methods Applied to the Brachistrone Problem",  
A. Jameson and J. Vassberg, Computational Fluid Dynamics, Journal, Vol. 9, No.3, Oct. 2000, pp. 281-296



# Computational Cost★

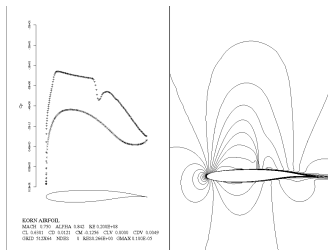
Total Computational Cost of Design		
+	Finite difference gradients Steepest descent	$\mathcal{O}(N^3)$
+	Finite difference gradients Quasi-Newton	$\mathcal{O}(N^2)$
+	Adjoint gradients Quasi-Newton	$\mathcal{O}(N)$
+	Adjoint gradients Smoothed gradient	$\mathcal{O}(K)$
Note: $K$ is independent of $N$ .		

★: "Studies of Alternative Numerical Optimization Methods Applied to the Brachistrone Problem",  
A. Jameson and J. Vassberg, Computational Fluid Dynamics, Journal, Vol. 9, No.3, Oct. 2000, pp. 281-296

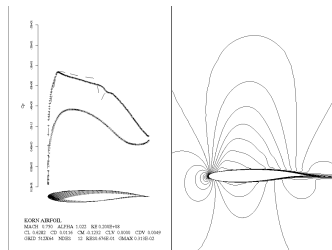
# DRAG MINIMIZATION



# Viscous Optimization of Korn Airfoil

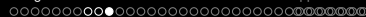


Initial

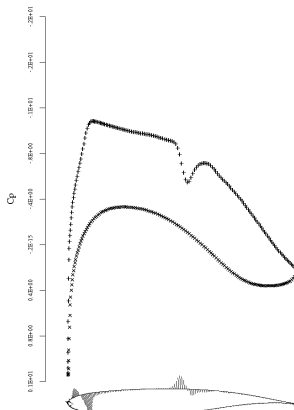


Final

Mesh size=512 x 64, Mach number=0.75,  $CL_{target}=0.63$ ,  
 Reynolds number=20 Million



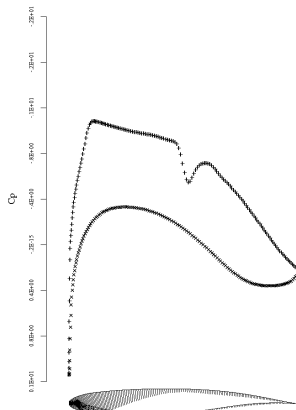
# The Effect of Applying Smoothed Gradient



KORN AIRFOIL

MACH 0.750 ALPHA 8.853 RE 0.250E+08  
 CL 5.6282 CD 0.0118 CM 0.1257 CLV 0.0000 CDV 0.0049  
 GRID 512X64 NDRE 1 RES0.284E+01 GMAX 6.555E-01

Unsmoothed



KORN AIRFOIL

MACH 0.750 ALPHA 8.853 RE 0.250E+08  
 CL 5.6282 CD 0.0118 CM 0.1257 CLV 0.0000 CDV 0.0049  
 GRID 512X64 NDRE 1 RES0.284E+01 GMAX 6.596E-02

Smoothed

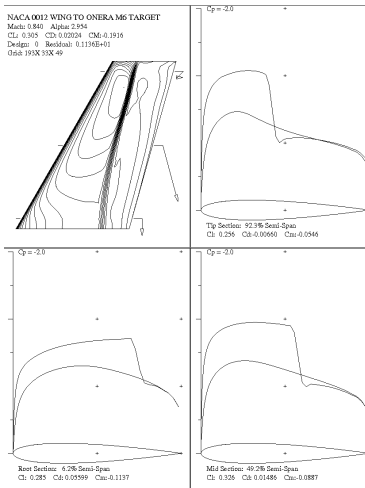
# INVERSE DESIGN

## Recovering of ONERA M6 Wing from its pressure distribution

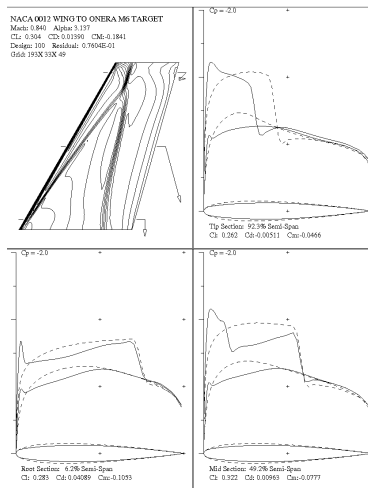
A. Jameson 2003–2004



# NACA 0012 WING TO ONERA M6 TARGET



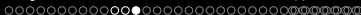
(a) Starting wing: NACA 0012



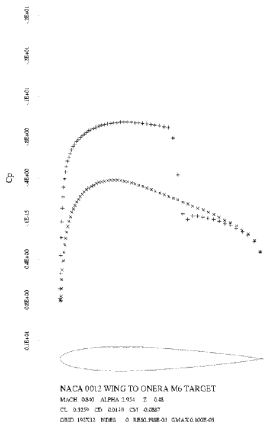
(b) Target wing: ONERA M6

This is a difficult problem because of the presence of the shock wave in the target pressure and because the profile to be recovered is symmetric while the target pressure is not.

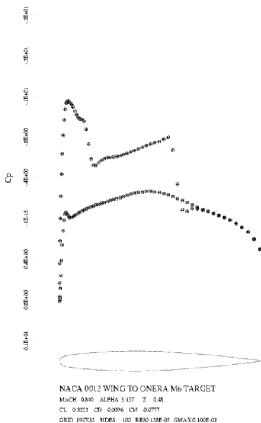




# Pressure Profile at 48% Span



(c) Staring wing: NACA 0012



(d) Target wing: ONERA M6

The pressure distribution of the final design match the specified target, even inside the shock.

# P51 RACER



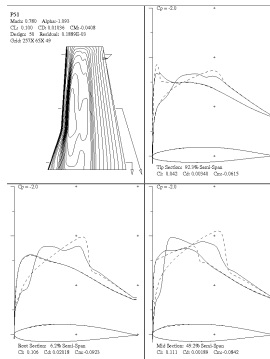
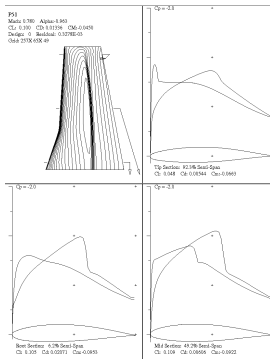
# P51 Racer



- Aircraft competing in the Reno Air Races reach speeds above 500 MPH, encountering compressibility drag due to the appearance of shock waves.
- Objective is to delay drag rise without altering the wing structure. Hence try adding a bump on the wing surface.

# Partial Redesign

- Allow only outward movement.
- Limited changes to front part of the chordwise range.

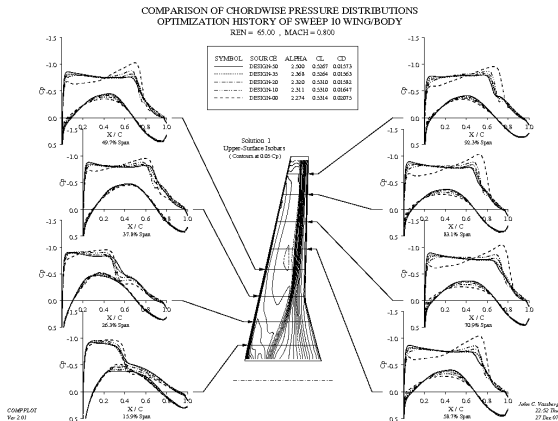


# DO WE NEED SWEPT WINGS ON COMMERCIAL JETS?

# Background for Studies of Reduced Sweep

- Current Transonic Transports
  - Cruise Mach:  $0.76 \leq M \leq 0.86$
  - C/4 Sweep:  $25^\circ \leq \Lambda \leq 35^\circ$
  - Wing Planform Layout Knowledge Base
    - Heavily Influenced By *Design Charts*
    - Data Developed From *Cut-n-Try* Designs
    - Data Aumented With Parametric Variations
    - Data Collected Over The Years
    - Includes Shifts Due To Technologies  
e.g., Supercritical Airfoils, Composites, etc.

# Pure Aerodynamic Optimizations



Evolution of Pressures for  $\Lambda = 10^\circ$  Wing during Optimization



# Pure Aerodynamic Optimizations

Mach	Sweep	$C_L$	$C_D$	$C_{D.tot}$	$ML/D$	$\sqrt{ML/D}$
0.85	35°	0.500	153.7	293.7	14.47	<b>15.70</b>
0.84	30°	0.510	151.2	291.2	14.71	<b>16.05</b>
0.83	25°	0.515	151.2	291.2	14.68	<b>16.11</b>
0.82	20°	0.520	151.7	291.7	14.62	<b>16.14</b>
0.81	15°	0.525	152.4	292.4	14.54	<b>16.16</b>
0.80	10°	0.530	152.2	292.2	14.51	<b>16.22</b>
0.79	5°	0.535	152.5	292.5	14.45	<b>16.26</b>

- $C_D$  in counts
- $C_{D.tot} = C_D + 140$  counts
- Lowest Sweep Favors  $\sqrt{ML/D} \simeq 4.0\%$

## Conclusion of Swept Wing Study

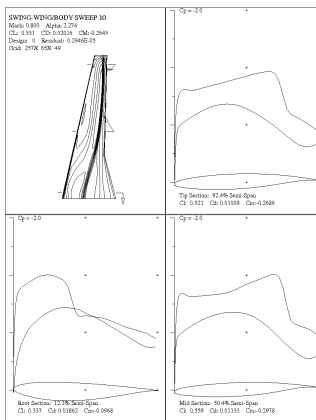
- An unswept wing at Mach 0.80 offers slightly better range efficiency than a swept wing at Mach 0.85.
- It would also improve TO, climb, descent and landing.
- Perhaps B737/A320 replacements should have unswept wings.

# DEMO OF LOW SWEEP DESIGN

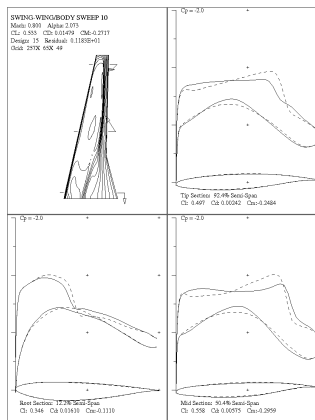




# Application II: Low Sweep Wing Redesign using RK-SGS Scheme



Initial



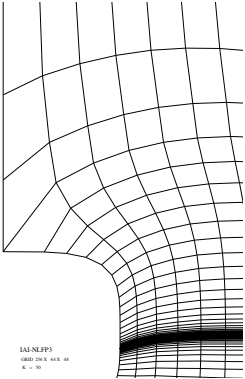
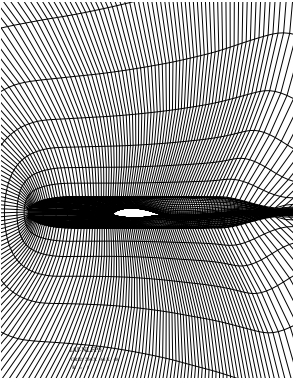
Final

Mesh size=256x64x48, Design Steps=15, Design variables=127x33=4191 surface mesh points

# WING DESIGN FOR NATURAL LAMINAR FLOW



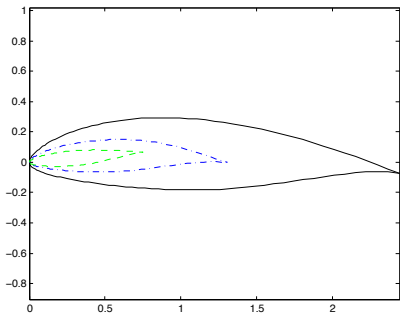
# Airplane Mesh



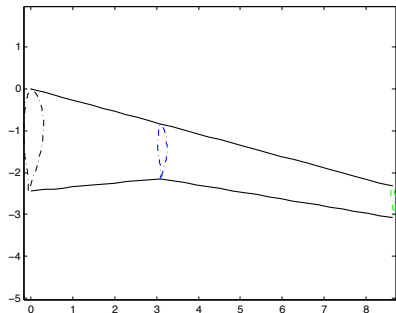
LAI-NL.FP3  
GRID 256 X 64 X 48  
N = 50

Mesh size=256x64x48

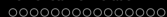
# Wing Planform and Sectional Profiles



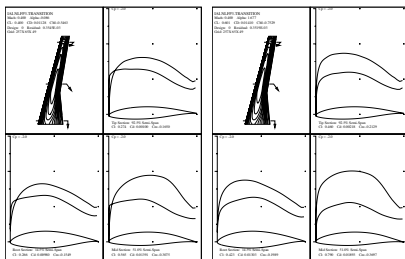
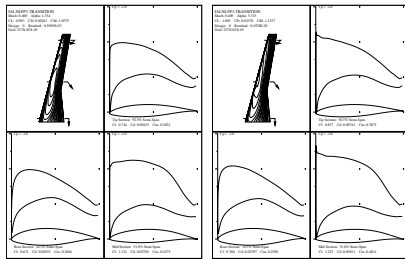
(a) Cross Sectional Profiles



(b) Wing Planform Shape



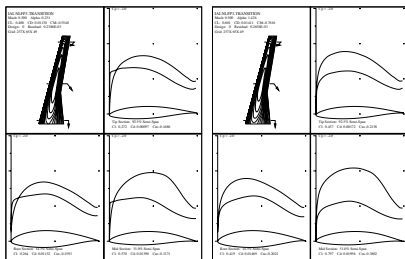
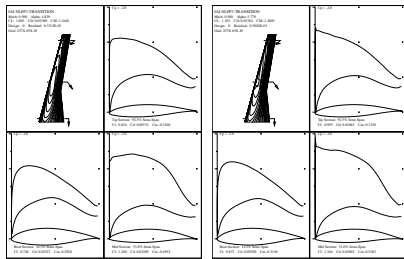
# Design Points: $M=0.40$ , $CL=0.4, 0.6, 0.9, 1.0$

(a)  $M=0.40$ ,  $CL=0.40$ (b)  $M=0.40$ ,  $CL=0.60$ (c)  $M=0.40$ ,  $CL=0.90$ (d)  $M=0.40$ ,  $CL=1.00$ 

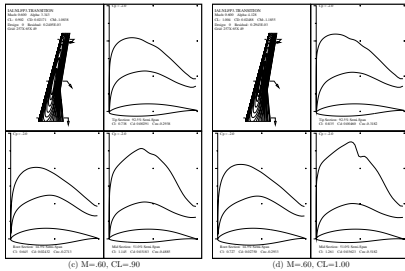
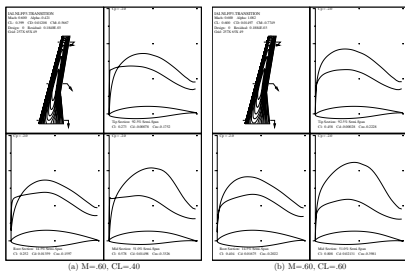
At  $M = .40$ , the lower limit of the operating range is set by the appearance of suction peak. This suction peak appears at the lower surface when  $CL < .40$ , and at the upper surface when  $CL > .90$ .



# Design Points: $M=0.50$ , $CL=0.4, 0.6, 0.9, 1.0$

(a)  $M=0.50$ ,  $CL=0.40$ (b)  $M=0.50$ ,  $CL=0.60$ (c)  $M=0.50$ ,  $CL=1.00$ (d)  $M=0.50$ ,  $CL=1.10$ 

At  $M = .50$ , the lower limit of the operating range is set by the appearance of suction peak. This suction peak appears at the lower surface when  $CL < .40$ , and at the upper surface when  $CL > 1.0$ .

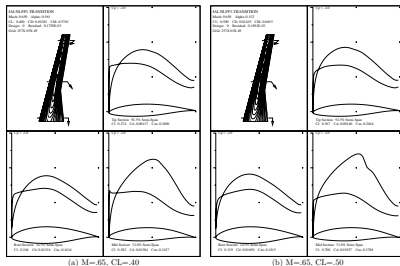
Design Points:  $M=0.60$ ,  $CL=0.4, 0.6, 0.9, 1.0$ 

At  $M = .60$ , the lower limit of the operating range is set by the appearance of suction peak at the lower surface, and the formation of shock at the upper surface. The suction peak appears at the lower surface when  $CL < .40$ , and the shock starts to form at the upper surface when  $CL > .90$ .



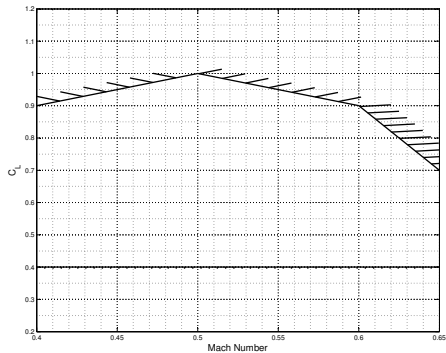


# Design Points: $M=0.65$ , $CL=0.4, 0.5$



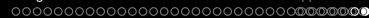
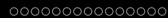
At  $M = .65$ , the lower limit of the operating range is set by the appearance of suction peak at the lower surface, and the formation of shock at the upper surface. The operating range has become too narrow to be useful. In particular, the suction peak appears at the lower surface when  $CL \leq 40$ , and the shock of moderate strength has already started to form at the upper surface when  $CL = .50$ .

# Operating Envelope (Limit) of Natural Laminar Flows

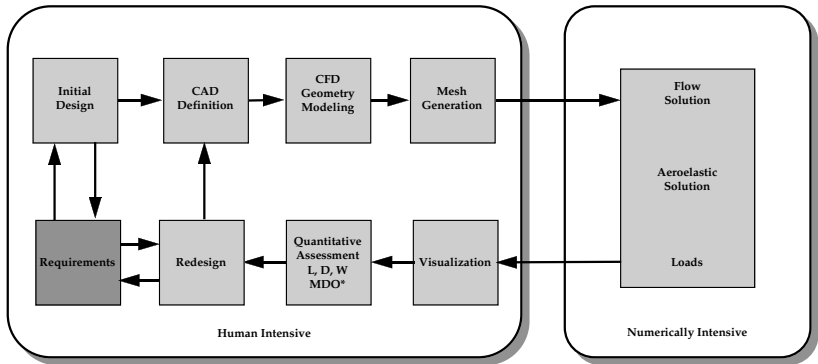


The figure shows the operating boundaries within which favorable pressure distribution can be maintained.

# NUMERICAL WIND TUNNEL

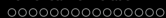


# Concept of Numerical Wind Tunnel



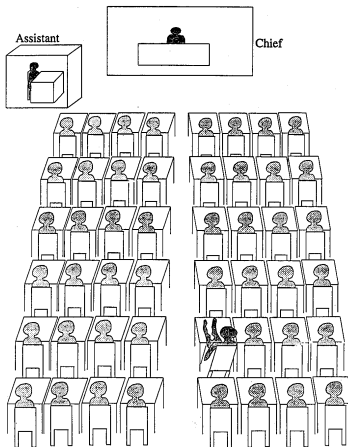
\*MDO: Multi-Disciplinary Optimization





## Traditional Engineering Offices

### Grumman Aerodynamics Section in 1968



# APPENDIX

# DESIGN USING THE TRANSONIC POTENTIAL FLOW EQUATION



# Airfoil Design For Potential Flow using Conformal Mapping

Consider the case of two-dimensional compressible inviscid flow. In the absence of shock waves, an initially irrotational flow will remain irrotational, and we can assume that the velocity vector  $\mathbf{q}$  is the gradient of a potential  $\phi$ . In the presence of weak shock waves this remains a fairly good approximation. Let  $p$ ,  $\rho$ ,  $c$ , and  $M$  be the pressure, density, speed-of-sound, and Mach number  $q/c$ . Then the potential flow equation is

$$\nabla \cdot (\rho \nabla \phi) = 0, \quad (19)$$

where the density is given by

$$\rho = \left\{ 1 + \frac{\gamma - 1}{2} M_\infty^2 (1 - q^2) \right\}^{\frac{1}{\gamma - 1}}, \quad (20)$$

while

$$p = \frac{\rho^\gamma}{\gamma M_\infty^2}, \quad c^2 = \frac{\gamma p}{\rho}. \quad (21)$$

Here  $M_\infty$  is the Mach number in the free stream, and the units have been chosen so that  $p$  and  $q$  have a value of unity in the far field.



## Airfoil Design For Potential Flow using Conformal Mapping

Suppose that the domain  $D$  exterior to the profile  $C$  in the  $z$ -plane is conformally mapped on to the domain exterior to a unit circle in the  $\sigma$ -plane. Let  $R$  and  $\theta$  be polar coordinates in the  $\sigma$ -plane, and let  $r$  be the inverted radial coordinate  $\frac{1}{R}$ . Also let  $h$  be the modulus of the derivative of the mapping function

$$h = \left| \frac{dz}{d\sigma} \right|. \quad (22)$$

Now the potential flow equation becomes

$$\frac{\partial}{\partial \theta} (\rho \phi_\theta) + r \frac{\partial}{\partial r} (r \rho \phi_r) = 0 \quad \text{in } D, \quad (23)$$

where the density is given by equation (20), and the circumferential and radial velocity components are

$$u = \frac{r \phi_\theta}{h}, \quad v = \frac{r^2 \phi_r}{h}, \quad (24)$$

while

$$q^2 = u^2 + v^2. \quad (25)$$

# Airfoil Design For Potential Flow using Conformal Mapping

The condition of flow tangency leads to the Neumann boundary condition

$$v = \frac{1}{h} \frac{\partial \phi}{\partial r} = 0 \text{ on } C. \quad (26)$$

In the far field, the potential is given by an asymptotic estimate, leading to a Dirichlet boundary condition at  $r = 0$ . Suppose that it is desired to achieve a specified velocity distribution  $q_d$  on  $C$ . Introduce the cost function

$$I = \frac{1}{2} \int_C (q - q_d)^2 d\theta,$$

## Design Problem

The design problem is now treated as a control problem where the control function is the mapping modulus  $h$ , which is to be chosen to minimize  $I$  subject to the constraints defined by the flow equations (19–26).

A modification  $\delta h$  to the mapping modulus will result in variations  $\delta\phi$ ,  $\delta u$ ,  $\delta v$ , and  $\delta\rho$  to the potential, velocity components, and density. The resulting variation in the cost will be

$$\delta I = \int_C (q - q_d) \delta q \, d\theta, \quad (27)$$

where, on  $C$ ,  $q = u$ . Also,

$$\delta u = r \frac{\delta\phi_\theta}{h} - u \frac{\delta h}{h}, \quad \delta v = r^2 \frac{\delta\phi_r}{h} - v \frac{\delta h}{h},$$

while according to equation (20)

$$\frac{\partial\rho}{\partial u} = -\frac{\rho u}{c^2}, \quad \frac{\partial\rho}{\partial v} = -\frac{\rho v}{c^2}.$$

## Design Problem

It follows that  $\delta\phi$  satisfies

$$L\delta\phi = -\frac{\partial}{\partial\theta}\left(\rho M^2\phi_\theta\frac{\delta h}{h}\right) - r\frac{\partial}{\partial r}\left(\rho M^2 r\phi_r\frac{\delta h}{h}\right)$$

where

$$L \equiv \frac{\partial}{\partial\theta}\left\{\rho\left(1 - \frac{u^2}{c^2}\right)\frac{\partial}{\partial\theta} - \frac{\rho uv}{c^2}r\frac{\partial}{\partial r}\right\} + r\frac{\partial}{\partial r}\left\{\rho\left(1 - \frac{v^2}{c^2}\right)r\frac{\partial}{\partial r} - \frac{\rho uv}{c^2}\frac{\partial}{\partial\theta}\right\}. \quad (28)$$

Then, if  $\psi$  is any periodic differentiable function which vanishes in the far field,

$$\int_D \frac{\psi}{r^2} L \delta\phi \, dS = \int_D \rho M^2 \nabla\phi \cdot \nabla\psi \frac{\delta h}{h} \, dS, \quad (29)$$

where  $dS$  is the area element  $r \, dr \, d\theta$ , and the right hand side has been integrated by parts.





## Design Problem

Equation (32) can be further simplified to represent  $\delta I$  purely as a boundary integral because the mapping function is fully determined by the value of its modulus on the boundary. Set

$$\log \frac{dz}{d\sigma} = \mathcal{F} + i\beta,$$

where

$$\mathcal{F} = \log \left| \frac{dz}{d\sigma} \right| = \log h,$$

and

$$\delta \mathcal{F} = \frac{\delta h}{h}.$$

Then  $\mathcal{F}$  satisfies Laplace's equation

$$\Delta \mathcal{F} = 0 \quad \text{in } D,$$

and if there is no stretching in the far field,  $\mathcal{F} \rightarrow 0$ . Introduce another auxiliary function  $P$  which satisfies

$$\Delta P = \rho M^2 \nabla \psi \cdot \nabla \psi \quad \text{in } D, \quad (33)$$

and

$$P = 0 \quad \text{on } C.$$

